Bi on the Si(001) surface

C. J. Kirkham, V. Brázdová, and D. R. Bowler
London Centre for Nanotechnology, 17-19 Gordon St, London, WC1H 0AH, United Kingdom and
Department of Physics and Astronomy, University College London, Gower St, London, WC1E 6BT, United Kingdom
(Received 18 January 2012; revised manuscript received 27 June 2012; published 30 July 2012)

The energetics and diffusion of Bi atoms on the Si(001) surface have been studied with density functional theory (DFT) to determine preferential adsorption sites. At several sites there is an unpaired electron on the Bi atom. Diffusion along the dimer rows at 300 K is very fast (10^6 to 10^{11} s^{-1}), with diffusion between rows considerably less so (10 s^{-1}). Multiple adatoms were found to react to form ad-dimers, in agreement with previous results.

DOI: 10.1103/PhysRevB.86.035328 PACS number(s): 68.35.bg, 31.15.A−, 68.43.Jk

I. INTRODUCTION

Silicon is an important material in the semiconductor industry, with its properties relying on the careful control of dopants. One class of dopants used are group V atoms, where traditionally the lighter elements, such as phosphorus, have been favored over the heavier ones, such as bismuth. However, in recent years, there has been an increased interest, both experimentally and theoretically, in the latter.[1–6] The heavier group V atoms have additional uses as surfactants for the Si(001) surface and their growth mechanisms have been studied.[7] With the increasing miniaturization of electronic circuits, there has been growing interest in the use of group V atoms as qubits for quantum computing.[8] For example, recent work has demonstrated the use of individual P atoms as transistors.[9] Bi is of particular interest due to its long electron spin coherence times and short decoherence times.[1] Previous work in this area has focused on bulk dopants rather than surface adatoms though.

The adsorption of single group V atoms has been studied in detail previously[10–12] up to Sb with the most complete work done on P. Group V atoms initially adsorb to the Si(001) surface as isolated adatoms and can adsorb at a variety of sites before forming dimers.

For phosphorus, it was found that isolated adatoms preferentially adsorb either at the M site, or near the D site (see Fig. 1 for labels), the former being more energetically favorable.[12] Through experimental observations[13] and theoretical calculations,[14] it was found that multiple adatoms favor adsorption as ad-dimers. For As and Sb, theoretical studies found preferential adsorption near the D site[11] and that adsorption of ad-dimers was favored over two isolated adatoms.[15] The presence of both As[16] and Sb[17] ad-dimers has been observed experimentally. There has been limited theoretical work on Bi adatoms so far,[18] usually focusing on dimers or larger structures, such as nanolines.[19–21]

Early experimental work[22] suggested that Bi mainly adsorbs on the Si(001) surface as dimers. Previous theoretical work on Bi adatoms[18] looked at the flat Si(001) 2 × 1 surface, which is not the correct surface reconstruction. These results supported adsorption as ad-dimers and suggested the D site as a preferential adatom site. Since then work has focused on ad-dimers looking at higher coverages of dimers,[23] and rotation and diffusion of these dimers.[24,25]

Here, we present an investigation of Bi adsorption and diffusion on Si(001) and Bi adatom properties. We also consider formation of ad-dimers.

II. METHODS

We used density functional theory (DFT)[26,27] with the gradient-corrected Perdew-Burke-Ernzerhof (PBE)[28] exchange-correlation functional as implemented in the Vienna *ab initio* simulation package (VASP)[29,30] version 4.6.34. For Bi, the $6s^2 6p^3$ electrons were treated as valence, the rest as core. The core electrons were described by the projector augmented wave (PAW) method.[31,32] An energy cutoff of 300 eV was used to converge the adsorption energies to within 0.01 eV.

The bulk lattice constant for silicon was calculated to be $a_0 = 5.469$ Å in very good agreement with the experimental value of 5.430 Å. This lattice constant was used throughout. The Si(001) surface was represented by a ten layer slab model with either $c(4 \times 2)$ or $p(2 \times 2)$ periodicity. The surface consists of two rows of four Si-Si dimers to prevent interaction between periodic images. The tenth layer was terminated by H atoms in a dihydride structure, and both the H atoms and the tenth layer of Si atoms were fixed. The Bi atoms were placed atop the first layer of Si atoms. The Bi and first nine Si layers were fully optimised. The periodic images were separated by a vacuum gap of 12.84 Å when no Bi was present.

A $(2 \times 2 \times 1)$ Monkhorst-Pack k-point mesh is adequate for coarse grained simulations but a $(3 \times 3 \times 1)$ k-point mesh was required to converge adsorption energies to within 0.01 eV for some sites. Geometry optimizations were performed with a 0.02 eV/Å convergence condition for the forces on each atom. All calculations were spin polarized.

Adsorption energy per Bi atom was calculated using

$$E_{\text{ads}} = \frac{E_{\text{surf+Bi}} - E_{\text{surf}} - nE_{\text{Bi}}}{n}, \tag{1}$$

where $E_{\text{surf+Bi}}$ is the energy of the structure with Bi adsorbed, E_{surf} is the energy of the clean surface, E_{Bi} is the energy of an atomic Bi calculated in the same unit cell, and n is the number of Bi atoms. To calculate the diffusion barriers and pathways between the different adatom sites, the climbing image nudged elastic band (CINEB) method[33] was used. Most calculations used three images, but for sites with considerably smaller or larger separations one or five images were used, respectively.

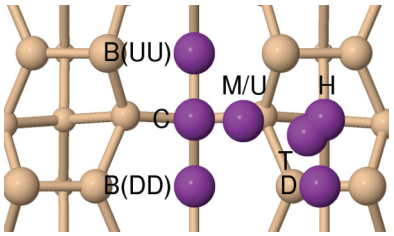

FIG. 1. (Color online) Top view of positions of adatom sites investigated on the $c(4 \times 2)$ surface. The letters indicate the label given to the sites in this paper. The M and U sites cannot be easily distinguished from a top view. Silicon is shown in beige (light color) and bismuth in purple (dark color). Atom sizes are scaled with height and only the first four layers are shown for clarity.

The rates of diffusion were calculated using

$$R = A \exp\left(\frac{-E_A}{k_b T}\right), \tag{2}$$

where A is the pre-exponential coefficient, here assumed to be 10^{13} s^{-1}, k_b is the Boltzmann constant, T is the temperature in Kelvin, and E_A is the activation energy.

III. RESULTS AND DISCUSSION

A. Adatoms

The adsorption sites for a single Bi adatom on the Si(001) $c(4 \times 2)$ and $p(2 \times 2)$ reconstructions have been investigated by optimizing the atomic structure of the system for multiple different starting geometries. Seven adsorption sites were found as shown in Fig. 1. Five of these correspond to structures from previous work for single adsorbates on the Si(001) surface, namely, B, D, H, M,[11,34] and C.[35] The remaining two, T and U, were identified in this work. Adsorption energies have been calculated for each site.

These sites can be split into two types, the on-row sites and the in-trench sites. The former includes the D, H, M, T, and U sites, the latter the B and C sites. Since the two surface

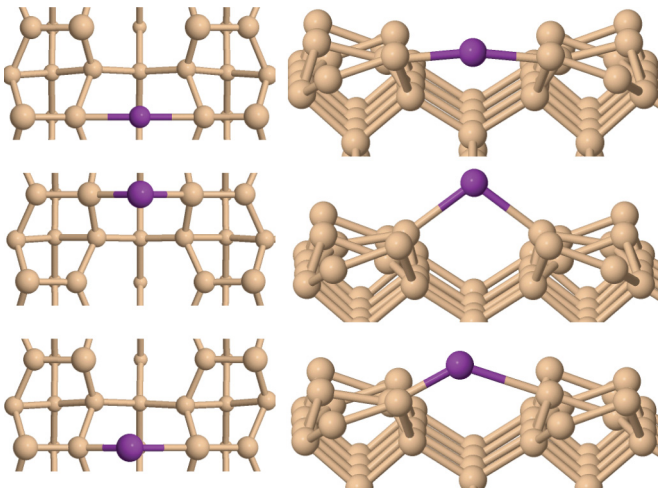

FIG. 2. (Color online) Top and side views of the B(DD)(top), B(UU)(middle) sites for the $c(4 \times 2)$ reconstruction, and B(bottom) site for the $p(2 \times 2)$ reconstructions.

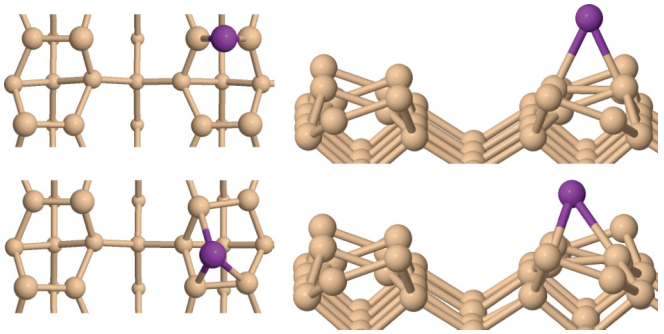

FIG. 3. (Color online) Top and side views of the D(top) and T(bottom) sites.

reconstructions are identical when looking at a single row, the on-row sites will be the same for both reconstructions, which was confirmed by initial calculations, whereas the in-trench sites will be affected by the different dimer arrangements across the rows. For the $p(2 \times 2)$ reconstruction, the dimer ends are always paired as an up and a down atom across the trench, whereas for the $c(4 \times 2)$ reconstruction, they can either be two up atoms or two down atoms. At all sites, the Bi adatom only had a significant effect on the geometry of the dimers it was directly bonded to. We now discuss the structure, properties, and energetics of these adsorption sites in detail: the in-trench sites in Sec. III A1, the on-row sites in Sec. III A2, their energies and spin in Sec. III A3, and bonding trends in Sec III A4.

1. In-trench sites

Site B is the bridge site between the ends of two dimers across the trench between rows, as shown in Fig. 2. Both B sites are identical for the $p(2 \times 2)$ reconstruction, but for the $c(4 \times 2)$ reconstruction there are two types, which have been labeled B(UU) and B(DD) due to the pairing of the surrounding Si dimer atoms. In these two cases, the Bi bonds to two Si atoms, but look significantly different due to the position of the Si atoms. The Bi-Si bond lengths are very similar (2.88 and 2.86 Å, respectively) but the B(UU) site has a much sharper Si-Bi-Si bond angle of 107.3°, whereas at the B(DD) site, it is nearly flat from one Si to the other with a bond angle of 170.4°. For the B(DD) structure, the Si dimers the Bi is attached to are lengthened by 0.04 Å, whereas for the B(UU), they are lengthened by 0.08 Å. On the $p(2 \times 2)$ surface, the Bi atom lies closer to the down atom (2.63 Å) than the up atom (3.18 Å), and lengthens the former Si dimer by 0.05 Å without changing the length of the latter. The bond to the up atom is only very weak. The Si-Bi-Si bond angle lies between those for the $c(4 \times 2)$ reconstruction structures at 133.8°.

Site C (not illustrated due to smaller adsorption energies) is the center site in the middle of the trench, which bonds weakly

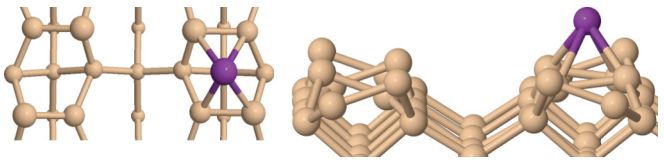

FIG. 4. (Color online) Top and side views of the H site.

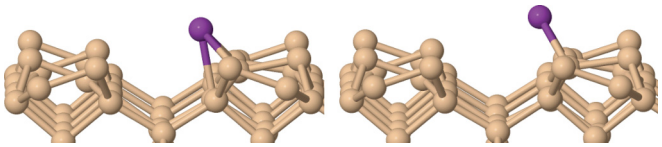

FIG. 5. (Color online) Side view of the M(left) and U(right) sites.

to the two surrounding up atoms. Due to the differences in buckling of the surface dimers the C site looks different for the two surface reconstructions. On the $p(2 \times 2)$ reconstruction, the Bi bonds diagonally, whilst on the $c(4 \times 2)$ reconstruction the Bi bonds between adjacent dimers separated by the trench. In both cases the four surrounding Si dimers are lengthened, those the Bi is bonded to by 0.06 Å, those it does not bond to by 0.09 Å.

2. *On-row sites*

Site D is located above a Si dimer, as shown in Fig. 3. The Bi is bonded to both Si atoms in the dimer, nearly flattening it and lengthening it by 0.01 Å. Since the dimer is not completely flat, the bonds to the former up atoms are slightly shorter (2.69 Å) than those to the formerly down atoms (2.71 Å). At site T, the Bi is three-fold coordinated, bonding to three surrounding Si atoms, as shown in Fig. 3, which has also been identified via calculations for group III adatoms.[11] The Bi bonds with two up atoms (2.94 and 2.86 Å, respectively), and one down atom (2.75 Å). The surrounding dimers were flattened slightly, but their bond lengths were unchanged to within 0.01 Å.

Site H is the pedestal site located between two dimers within a row. Here the Bi bonds to four surrounding Si atoms and partly flattens both surrounding dimers, as shown in Fig. 4. As with the D site, bonds with the formerly up atoms are shorter (2.88 Å compared to 2.94 Å). The Si dimers directly attached to the Bi are lengthened by 0.05 Å.

Sites M and U are very similar to each other, both being interdimer sites located above a second layer Si and between the ends of dimers within a row as shown in Fig. 5. The main difference between the two is the height at which the Bi lies above the surface. The M site lies 2.77 Å above the second layer Si, whereas the U site is 3.26 Å above it. At the M site, the Bi bonds to three Si atoms, two dimer ends and the second layer Si directly below it, whereas at the U site the Bi only bonds to the two dimer ends. The lack of charge density between the Bi atom and the subsurface Si indicates that at the U site there is no bond between these two atoms. At both sites, the bond to the formerly up atom is shorter than that to the formerly down atom and at the M site the bond to the second layer Si is the longest. At the M site, the Si dimer at the down end is shortened by 0.02 Å and the dimer at the up end is lengthened by 0.04 Å, whereas for the U site, the former dimer is unchanged, whilst the latter is lengthened by 0.07 Å. The U site is similar to the elevated end bridge structure seen during P diffusion on the same surface.[12]

TABLE I. Adsorption energies of the different sites on both the $c(4 \times 2)$ and $p(2 \times 2)$ reconstructed surfaces, with overall spin fixed to 0 and 1/2.

	Spin (μ_B)	
	0	1/2
Site	E_{ads} (eV)	E_{ads} (eV)
$c(4 \times 2)$		
B(DD)	−1.23	−1.20
B(UU)	−1.76	−1.84
C	−1.31	−1.30
D	−2.45	−2.61
H	−2.44	−2.40
M	−2.53	−2.49
T	−2.62	−2.59
U	−2.24	−2.38
$p(2 \times 2)$		
B	−1.40	−1.55
C	−1.43	−1.47

3. *Adsorption energies and spin*

Results where the overall spin on the adsorbed system is fixed to either 0 or 1/2 are presented in Table I. In both cases, E_{ads} is calculated with regards to the same E_{surf} and E_{Bi}. The $p(2 \times 2)$ on-row structures are the same as the $c(4 \times 2)$ structures, and therefore they are not shown.

On-row sites have a larger adsorption energy than the in-trench sites, by more than 1 eV in some cases. Spin makes little difference to the geometries of the different structures, but plays an important role in determining the energies. For the B(UU), D, U, and $p(2 \times 2)$ B and C sites, having an overall spin of 1/2 is more energetically favorable. For every other adsorption site forcing a spin of 1/2 on the system reduces the adsorption energy compared to no overall spin. As Fig. 6 shows, for the B(UU), D, and U sites, there is an unpaired electron on the Bi atom, which is of interest in applications where spin is important. The common feature between these sites is the fact that the Bi is twofold coordinated, whereas for the other sites, the Bi is threefold coordinated or more. Structures

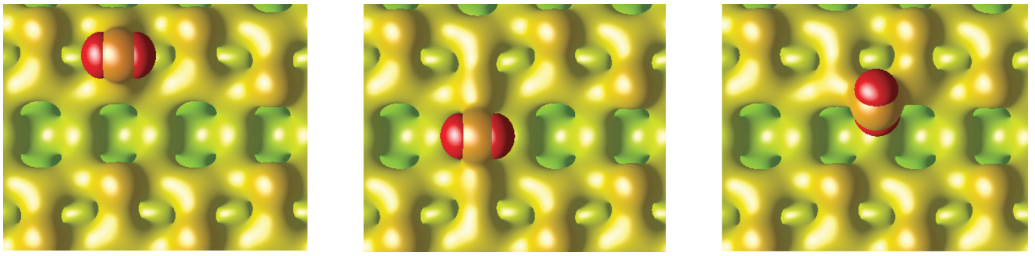

FIG. 6. (Color online) Spin density difference and charge density for a Bi at the D (left), B(UU) (middle), and U (right) sites, showing an unpaired electron on the Bi atom. Red indicates spin up and other colors charge density colored by height. The dimer rows run from left to right.

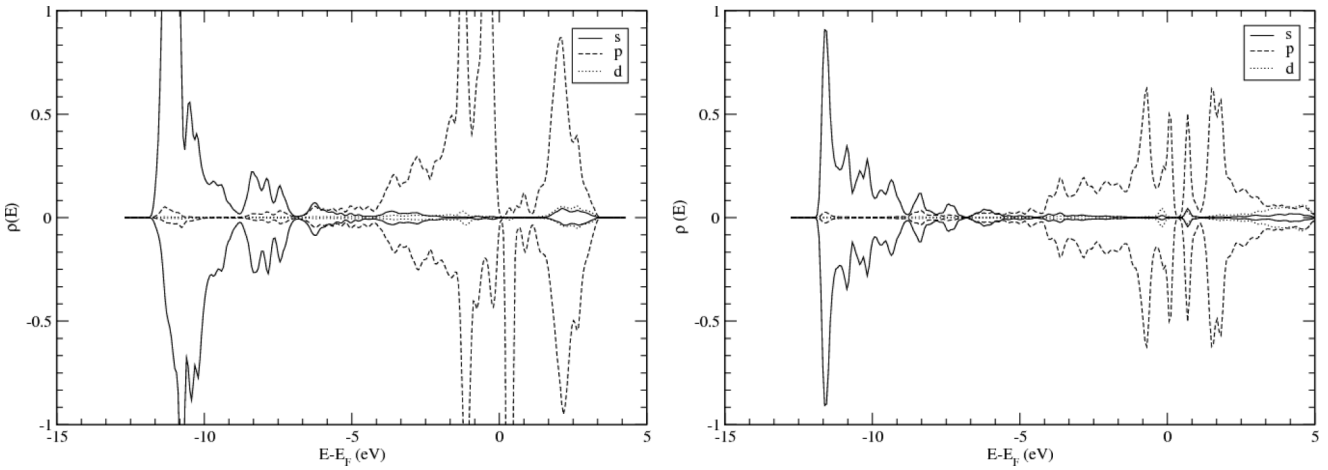

FIG. 7. *spd*-orbital decomposed density of states (DOS) plots for the D(left) and H(right) site Bi atom. Plots are scaled to the same height to allow for direct comparison. The unbroken lines are *s* orbitals, dashed are *p* orbitals, and dotted are *d* orbitals. The spin-majority DOS are plotted on the positive $\rho(E)$ axis, the spin minority on the negative.

where the Bi is twofold coordinated with bond angles near 90° show spin, and this arises due to the natural Bi bonding being p^3 rather than sp^3.[20] The importance of the bond angle is demonstrated by the B(DD) structure where no spin is more energetically favourable than 1/2 spin, despite being twofold coordinated. In the latter case, the spin is split between the Bi atom and the two Si atoms it is directly bonded to. This change in electronic structure can be explained by the change in hybridisation due to the much larger Si-Bi-Si bond angle of 170.4°. The D site is unusual in that the bond angle is only 52.2° and yet it shows spin on the Bi.

Using the D site as a test case we determined that spin-orbit coupling does not have a significant impact on the energetics of these structures. The largest energy difference observed was only 3 meV, comparing the field aligned along the *x* and *z* directions.

There is little agreement between the results of this work and those previously obtained.[18] The previous work used an atomic cluster model featuring flat dimers, which do not represent the real structure, and most of the differences can be attributed to this fact. There is disagreement in the ordering of the sites in terms of adsorption energy and significant quantitative differences in calculated adsorption energies for all but the H site. The difference in geometries between the flat and buckled surfaces alters how favourable certain sites are, especially for those bridging the trench. This may explain the large differences seen for the B and C sites and why the structures such as the T site were not investigated previously.

DFT is likely to predict the sites where a single unpaired electron is on the Bi to be less stable than they actually are due to the self interaction problem. There are several methods for addressing this problem, such as including exact exchange, using DFT + U or self interaction correction. However, all of these solutions require some degree of empiricism and the only effect that these would have would be to make these structures even more stable.

4. Bonding trends

By analyzing the *spd*-orbital decomposed density of states (DOS) for the Bi adatoms at the different sites, information on the nature of their bonding can be obtained. There are some general trends in Bi bonding shared across all adsorption sites, but there are also some striking differences between sites with and without an unpaired electron. The *s* states are mostly populated at energies 10 to 12 eV below the Fermi energy (E_F) with only small populations close to or above E_F. This shows that the *s* states of the Bi play little role in the bonding process. For structures without an unpaired electron, these *s* states are sharper and deeper, lying closer to 12 eV below E_F,

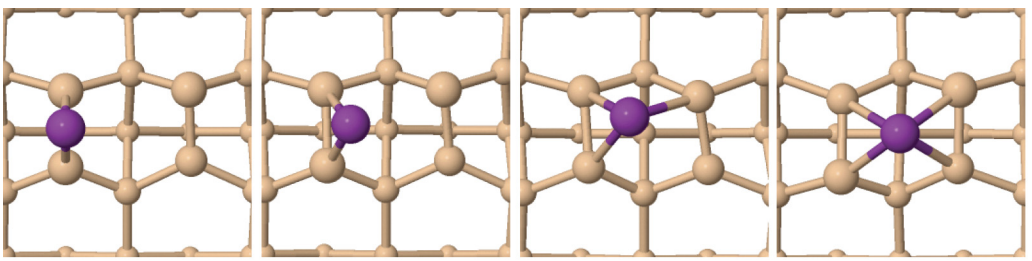

FIG. 8. (Color online) Diffusion pathway from the D site (far left) to the H (far right). The energies given are relative to the D site. The H site is a transition state between two T sites on opposite corners of the two dimer block.

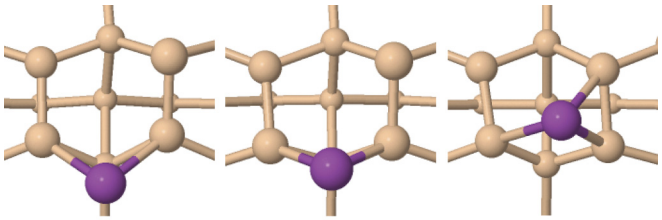

FIG. 9. (Color online) Diffusion pathway from the M (left) to the T (right) sites. The energies given are relative to the M site. The intermediate U site does not have spin on the Bi atom.

whilst those with an unpaired electron are usually more spread out and closer to 11 eV below E_F.

For the p states, the largest populations are around E_F, showing that it is mainly the p electrons that participate in bonding. For those structures, where there is an unpaired electron on the Bi atom, there is a sharp peak in the spin majority DOS just below E_F and a sharp peak in the spin minority DOS just above E_F, indicating that the unpaired electron is in a p orbital. As such the B(UU), D, and U sites all have a similar DOS.

The D, H, and T sites are in similar positions on the dimer row, but the bonding at the D site is significantly different from that at the H and T sites, as demonstrated in Fig. 7. The spin splitting seen in the D site DOS indicates that there is a single p orbital that can not be involved in bonding, meaning the bonding is either sp^2 or p^3. Given the depth of the s orbital, p^3 bonding is likely to be stronger. Whereas the H and T sites do not show this splitting which indicates sp^3 bonding is involved. Differences between the M and U site DOS confirm that the two structures have different bonding, despite the Bi being in very similar positions. The M site has s states that are 1 eV deeper, whilst the U site has more populated p states around E_F and shows the spin splitting characteristic of an unpaired electron.

B. Diffusion

Diffusion of the Bi atoms can either occur on the dimer rows (see Sec. III B1) or in the trench (see Sec. III B2). In both cases, the Bi can either diffuse parallel or perpendicular to the direction of the feature. For diffusion on the rows, both reconstructions are considered the same, so only the $c(4 \times 2)$ reconstruction is investigated. For diffusion through the trench, both the $c(4 \times 2)$ and $p(2 \times 2)$ reconstructions are investigated. A brief discussion of diffusion rates is presented in Sec. III B3.

1. Diffusion on the dimer rows

The route from one D site to another involves diffusion from a D site to the nearest T site, through the H site to the opposite T site before reaching the next D site along the row, as shown in Fig. 8. The activation energy for diffusion from a D site to a T site is 0.07 eV in the forward and 0.09 eV in the reverse direction. The H site was revealed to be a metastable intermediate between two T sites, as such an activation energy of 0.18 eV is required to move between T sites. The limiting step for diffusion along the rows is therefore diffusing between the T sites.

Diffusion across the rows, between the sites that lie on the edge of the row and those in the center, as shown in Fig. 9, was investigated to find out whether the Bi was more likely to move towards the trench or stay in the middle of the dimer rows. Diffusion from the M site to the T site showed subtleties related to spin. The U site with zero magnetic moment appeared as an intermediate on the path, which is 0.13 eV less stable than the U site with spin 1/2. Clearly small changes in bonding can have a strong effect on the spin state of the Bi. There was a 0.29 eV activation energy for moving from M to T and a 0.37 eV activation energy moving in the reverse direction. Diffusion away from the trench is therefore easier than diffusion towards the trench. Diffusion to all other on-row sites had to go via the T site first.

2. Diffusion in the trench

Diffusion in the trench can either occur across or along the trench. For diffusion across the trench several different routes were considered. The starting point was either taken to be a D or M site and the end point was considered to be a B, C, or M site, with the M site on the opposite end of the trench. Since the B site is not symmetric on the $p(2 \times 2)$ reconstruction, diffusion from both sides of the trench must be considered.

For the $c(4 \times 2)$ reconstruction, diffusion from a D site to a B(UU) site is in a straight line between the two sites, with the Bi moving through intermediate structures where it is only bonded to a single Si. This has an activation energy of

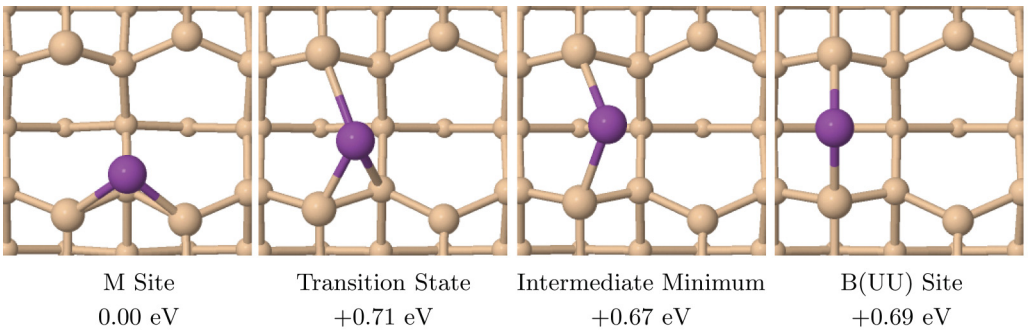

FIG. 10. (Color online) Diffusion pathway across the trench from an M (left) to the B(UU) (right) sites. The energies given are relative to the M site. The route up to the third image also serves as the diffusion pathway across the trench between two M sites.

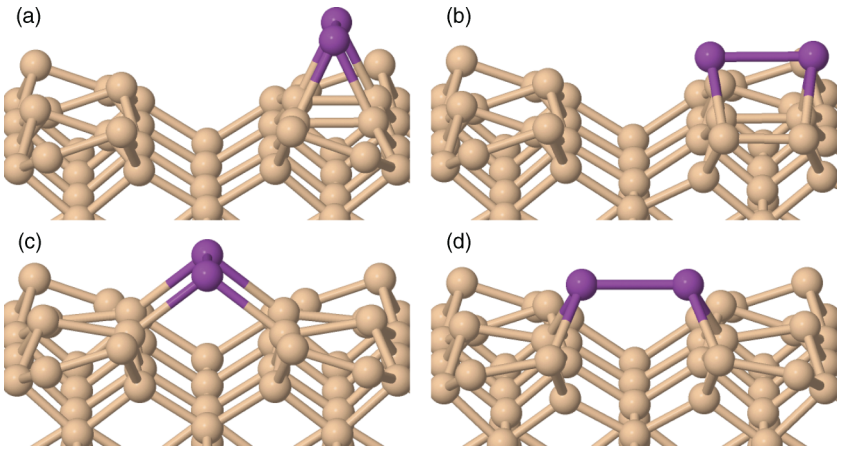

FIG. 11. (Color online) Bi ad-dimers on the Si(001) $c(4 \times 2)$ surface, (a) dimer at DD position, (b) dimer at UU position, (c) dimer at BB position, and (d) dimer at MM position.

1.32 eV, whereas the reverse process has an activation energy of 0.55 eV. Diffusion between the D and B(DD) sites goes via an M site first. The B(DD) site was revealed to be a metastable intermediate between two M sites, as such an activation energy of 1.30 eV is required to reach the B(DD) site. Diffusion between the M site and the B(UU), as shown in Fig. 10, is via an intermediate minimum with nearly the same energy as the B(UU) site. Here, the Bi is out of line with the up atoms, parallel to the direction of the trench. The activation energy for the first step is 0.71 eV, whereas the reverse is only 0.04 eV. The activation energy for diffusion between the intermediate and the B(UU) site is only 0.02 eV. Finally, the C site is shown to be a metastable intermediate with an activation energy of 1.22 eV coming from the M site. These activation energies show that for diffusion between the rows the route between two M sites via the B(UU) site would be most favourable due to its lower activation energy, and that diffusion out of the trench is more favourable than diffusion into the trench. A calculation of the full M to M diffusion path confirmed this, and found the Bi to diffuse via the intermediate minimum in Fig. 10, bypassing the B(UU) site.

For the $p(2 \times 2)$ reconstruction, diffusion between the rows is complicated by the fact the in-trench sites are asymmetric, however, this has little overall effect on the diffusion pathways across the trench. As with the $c(4 \times 2)$ reconstruction, the pathway with the lowest activation barrier lies between the B and C sites, and is higher in energy at 0.84 eV.

Diffusion along the trench will occur in a similar manner to diffusion across the trench, going via the M and B sites. This is because the C site lies higher in energy than the intermediate on the M to B path, so diffusion down the center of the trench will have a higher energy barrier than diffusion between adjacent M sites.

TABLE II. Adsorption energies per Bi atom for Bi ad-dimers on the $c(4 \times 2)$ Si(001) surface, labeled as in Fig. 11.

Ad-dimer	E_{ads}/Bi atom(eV)
DD	−3.38
UU	−3.24
MM	−2.88
BB	−2.85

3. *Diffusion rates*

Diffusion along the rows is much faster than diffusion between the rows. For example, at 300 K, diffusion between the on-row sites have rates ranging from 10^6 to 10^{11} s^{-1} whereas the diffusion rate for the most favourable route across the trench is only of order 10 s^{-1}. To observe Bi adatoms, diffusion would need to be suppressed. Cooling to below 20 K would be required to reduce all diffusion rates to at least 10^{-5} s^{-1} (of the order of 1 per day) and allow the use of these structures experimentally, with further cooling needed for use in devices.

C. Ad-dimers

Most observations of high coverages of Bi on Si(001) show dimers.[19] We therefore calculated the relative stabilities of dimers compared to adatoms. Four different ad-dimer structures were studied, here labeled DD, UU, MM, and BB, as shown in Fig. 11, indicating the location of the two adatoms in relation to the adatom sites used. Other configurations were not considered on the basis of stability and in light of experimental observations. The adsorption energy per Bi atom for each structure is presented in Table II.

In line with experimental observations and following chemical intuition, ad-dimer structures were found to be more energetically favorable than two adatoms at equivalent sites. The DD ad-dimer is the most energetically favorable, as found previously.[18,20] The diffusion rates for Bi adatoms indicate that dimers would preferentially form on rows, though MM dimers might form if two Bi atoms on adjacent rows bonded. This means that two Bi adatoms on the Si(001) surface would form an ad-dimer rather than remain as two separated adatoms, given temperatures above 20 K and enough time.

IV. CONCLUSIONS

We have shown that Bi adatoms will preferentially adsorb on the Si dimer rows, rather than in the trench between them. The most energetically favorable sites are the D and T sites. The D, U, and B(UU) sites have an unpaired electron on the Bi atom. Diffusion of the Bi atoms on the Si(001) surface at 300 K was found to be fast in all directions, with diffusion along the Si dimer rows (10^6 to 10^{11} s^{-1}) several orders of magnitude faster than diffusion between rows (10 s^{-1}). Finally, two adatoms will preferentially form an ad-dimer.

The D, U, and B(UU) sites are all potential qubit candidates due to the unpaired electron on their Bi atoms. Of these the D site is the most promising due to its large adsorption energy. However, the low activation energies for diffusion and the preference for forming ad-dimers means that experimental observation of these structures could prove difficult. The Bi would either diffuse away quickly into the rest of the surface, or pair up with other Bi atoms moving around the surface to form ad-dimers. This explains the lack of reported experimental observations of Bi adatoms on Si(001) even at low coverages (∼0.05 ML),[24] since very low coverages and temperatures would be required to prevent dimer formation. Even if low enough temperatures and coverages were used, there is no guarantee that the Bi would adsorb at the desired sites. This suggests that the utility of Bi on the clean Si(001) surface for QIP applications is limited. However, we are actively investigating schemes to isolate individual Bi atoms by modifying the surface, which will be presented in a future publication.

ACKNOWLEDGMENTS

The authors acknowledge the use of the UCL Legion High Performance Computing Facility, and associated support services, in the completion of this work. The authors acknowledge the useful discussions with Kazushi Miki, Katsuya Iwaya, Gabriel Aeppli, Steven Schofield, Philipp Studer, and Neil Curson. C. J. Kirkham is funded through a UCL Impact Studentship.

[1] G. W. Morley, M. Warner, A. M. Stoneham, P. T. Greenland, J. van Tol, C. W. M. Kay, and G. Aeppli, Nat. Mater. **9**, 725 (2010).
[2] M. H. Mohammady, G. W. Morley, and T. S. Monteiro, Phys. Rev. Lett. **105**, 067602 (2010).
[3] R. E. George, W. Witzel, H. Riemann, N. V. Abrosimov, N. Nötzel, M. L. W. Thewalt, and J. J. L. Morton, Phys. Rev. Lett. **105**, 067601 (2010).
[4] T. Sekiguchi, M. Steger, K. Saeedi, M. L. W. Thewalt, H. Riemann, N. V. Abrosimov, and N. Nötzel, Phys. Rev. Lett. **104**, 137402 (2010).
[5] M. Belli, M. Fanciulli, and N. V. Abrosimov, Phys. Rev. B **83**, 235204 (2011).
[6] M. H. Mohammady, G. W. Morley, A. Nazir, and T. S. Monteiro, Phys. Rev. B **85**, 094404 (2012).
[7] K. Sakamoto, K. Kyoya, K. Miki, H. Matsuhata, and T. Sakamoto, Jpn. J. Appl. Phys. Lett. **32**, L204 (1993).
[8] B. E. Kane, Nature **393**, 133 (1998).
[9] M. Fuechsle, J. A. Miwa, S. Mahapatra, H. Ryu, S. Lee, O. Warschkow, L. C. L. Hollenberg, G. Klimeck, and M. Y. Simmons, Nat. Nanotechnology **7**, 242 (2012).
[10] N. Takeuchi, Phys. Rev. B **63**, 035311 (2000).
[11] N. Takeuchi, Surf. Sci **482**, 44 (2001).
[12] J. M. Bennett, O. Warschkow, N. A. Marks, and D. R. McKenzie, Phys. Rev. B **79**, 165311 (2009).
[13] Y. Wang, X. Chen, and R. J. Hamers, Phys. Rev. B **50**, 4534 (1994).
[14] P. Sen, B. Gupta, and I. Batra, Phys. Rev. B **73**, 085319 (2006).
[15] S. Tang and A. J. Freeman, Phys. Rev. B **48**, 8068 (1993).
[16] R. D. Bringans, D. K. Biegelsen, and L.-E. Swartz, Phys. Rev. B **44**, 3054 (1991).
[17] M. Richter *et al.*, Phys. Rev. Lett. **65**, 3417 (1990).
[18] S. Tang and A. J. Freeman, Phys. Rev. B **50**, 1701 (1994).
[19] K. Miki, J. H. G. Owen, D. R. Bowler, G. A. D. Briggs, and K. Sakamoto, Surf. Sci **421**, 397 (1999).
[20] D. R. Bowler, Phys. Rev. B **62**, 7237 (2000).
[21] J. H. G. Owen, K. Miki, and D. R. Bowler, J. Mater. Sci. **41**, 4568 (2006).
[22] H. Noh, C. Park, D. Jeon, K. Cho, T. Hashizume, Y. Kuk, and T. Sakurai, J. Vac. Sci. Technol. B **12**, 2097 (1994).
[23] S. Gay, S. Jenkins, and G. Srivastava, Surf. Sci **402**, 641 (1998).
[24] S. Bulavenko, I. Koval, P. Melnik, N. Nakhodkin, and H. Zandvliet, Surf. Sci **482-485**, 370 (2001).
[25] K. Chuasiripattana and G. P. Srivastava, Phys. Rev. B **71**, 153312 (2005).
[26] P. Hohenberg and W. Kohn, Phys. Rev. **136**, B864 (1964).
[27] W. Kohn and L. J. Sham, Phys. Rev. **140**, A1133 (1965).
[28] J. Perdew, K. Burke, and M. Ernzerhof, Phys. Rev. Lett. **77**, 3865 (1996).
[29] G. Kresse and J. Hafner, Phys. Rev. B **48**, 13115 (1993).
[30] G. Kresse and J. Furthmüller, Phys. Rev. B **54**, 11169 (1996).
[31] P. E. Blöchl, Phys. Rev. B **50**, 17953 (1994).
[32] G. Kresse and D. Joubert, Phys. Rev. B **59**, 1758 (1999).
[33] G. Henkelman, B. Uberuaga, and H. Jonsson, J. Chem. Phys. **113**, 9901 (2000).
[34] G. Brocks, P. J. Kelly, and R. Car, Surf. Sci **269-270**, 860 (1992).
[35] A. M. P. Sena and D. R. Bowler, J. Phys.: Condens. Matter **23**, 305003 (2011).